Cancer Cell
Article

Stat3/Socs3 Activation by IL-6 Transsignaling Promotes Progression of Pancreatic Intraepithelial Neoplasia and Development of Pancreatic Cancer

Marina Lesina,[1] Magdalena U. Kurkowski,[1] Katharina Ludes,[1] Stefan Rose-John,[2] Matthias Treiber,[1] Günter Klöppel,[3] Akihiko Yoshimura,[4] Wolfgang Reindl,[1] Bence Sipos,[5] Shizuo Akira,[6] Roland M. Schmid,[1,*] and Hana Algül[1,*]
[1]II. Medizinische Klinik, Klinikum rechts der Isar, Technische Universität München, 81675 Munich, Germany
[2]Institute of Biochemistry, Christian-Albrechts-University of Kiel, 24098 Kiel, Germany
[3]Institute of Pathology, Technische Universität München, 81675 Munich, Germany
[4]Department of Microbiology and Immunology, Keio University School of Tokyo, and Japan Science and Technology Agency (JST), CREST, Chiyoda-ku, 102-0075 Tokyo, Japan
[5]Department of Pathology, Universitätsklinikum Tübingen, 72076 Tübingen, Germany
[6]Laboratory of Host Defense, WPI Immunology Frontier Research Center, Osaka University, 565-0871 Osaka, Japan
*Correspondence: hana.alguel@lrz.tum.de (H.A.), roland.schmid@lrz.tum.de (R.M.S.)
DOI 10.1016/j.ccr.2011.03.009

SUMMARY

Physiological levels of $Kras^{G12D}$ are sufficient to induce pancreatic intraepithelial neoplasias (PanINs); the mechanisms that drive PanIN progression are unknown. Here, we establish that, in addition to oncogenic $Kras^{G12D}$, IL-6 transsignaling-dependent activation of Stat3/Socs3 is required to promote PanIN progression and pancreatic ductal adenocarcinoma (PDAC). Myeloid compartment induces Stat3 activation by secreting IL-6; consequently, IL-6 transsignaling activates Stat3 in the pancreas. Using genetic tools, we show that inactivation of IL-6 transsignaling or Stat3 inhibits PanIN progression and reduces the development of PDAC. Aberrant activation of Stat3 through homozygous deletion of *Socs3* in the pancreas accelerates PanIN progression and PDAC development. Our data describe the involvement of IL-6 transsignaling/Stat3/Socs3 in PanIN progression and PDAC development.

INTRODUCTION

Despite the considerable efforts that have been made in basic and clinical research, pancreatic ductal adenocarcinoma (PDAC) affects 230,000 patients in the Western Hemisphere annually. PDAC is notable for its high mortality, constituting the fourth leading cause of death due to cancer (Hidalgo, 2010).

Recent efforts have helped identify the molecular genetic determinants of PDAC. Activating *KRAS* mutations have been detected in 30% of pancreatic intraepithelial neoplasias (PanINs), which are precursor lesions, increasing to 100% in advanced PDACs. Inactivation of *INK4A* and *TRP53* occurs later during PanIN progression and PDAC formation (Hruban et al., 2006).

These findings have been mirrored in mouse models. Pancreas-specific expression of mutations ($Kras^{G12D}$, $Kras^{G12V}$, $Kras^{G12D}$, $Trp53^{R172H}$) or deletion of tumor suppressor genes (*Trp53*, *Ink4A/Arf*) in genetically engineered mice (GEM) recapitulates PanIN initiation and progression to pancreatic cancer (PC), similar to the clinical pathology (Aguirre et al., 2003; Guerra et al., 2007; Hingorani et al., 2003, 2005; Kelly et al., 2008). Although it has been studied in GEM for pancreatic cancer, the role of concomitant stromal reactions (stromal desmoplasia) in PanIN progression and cancer development has not been addressed; most existing concepts have merely been inferred.

The presence of stromal desmoplasia is a hallmark of PDAC (Algul et al., 2007b), forming a unique microenvironment that comprises many cell types, including proliferating fibroblasts and pancreatic stellate cells that produce and deposit fibronectin and collagen, and inflammatory cells and macrophages that release chemokines and cytokines. In particular, the function of concomitant inflammation in PDAC has garnered recent interest, because proinflammatory markers in the serum, such

Significance

Despite the availability of current multimodal therapies, treatment outcomes in pancreatic ductal adenocarcinoma (PDAC) are poor, generating overall survival rates of less than 5%. Late diagnosis, early metastasis, and the lack of a specific therapy contribute to this dismal prognosis. Although genetic studies have observed that activating *Kras* mutations are the initial, frequently occurring genetic alterations, signaling pathways that drive PanIN progression have not been described. In this study, we implicate the IL-6 transsignaling/Stat3/Socs3 pathway as an important mediator of PanIN progression and PDAC development.

as interleukin (IL)-1β and IL-6, are associated with outcomes in PDAC (Ebrahimi et al., 2004; Sawai et al., 2003). Additionally, chronic pancreatitis is a risk factor for PDAC, supporting the involvement of concomitant inflammation in pancreatic oncogenesis (Lowenfels et al., 1993).

Dysregulated activation of **s**ignal **t**ransducer and **a**ctivator of **t**ranscription (Stat) family members occurs often in many human malignancies. Of the seven Stat proteins, activation of Stat3 in cancer is related to tumor growth directly through tumor-autonomous mechanisms and indirectly by modulating tumor-associated stroma and the immune system. Activation depends on the phosphorylation of a conserved tyrosine residue (Y705) by upstream kinases, such as Janus kinase 2 (Jak2). Jak2 activation requires activation of the ubiquitously expressed gp130 receptor by specific ligands (IL-6, leukemia inhibitor factor [LIF], IL-11, oncostatin M [OSM], ciliary neurotrophic factor [CNTF], IL-27).

Of these ligands, IL-6 has the unique capacity to activate Stat3 using two modes. The first mode entails classical signaling mechanisms, characterized by the binding of IL-6 to the IL-6 receptor (IL-6R) and gp130 on specific target cells. However, a few subsets of cells, such as monocytes/macrophages and hepatocytes, express the membrane-bound IL-6R, whereas gp130 is ubiquitously expressed. Alternatively, IL-6 binds to a naturally occurring soluble form of IL-6R (sIL-6R), forming a complex that induces IL-6-specific signaling in cells that lack membrane-bound IL-6R, a process that is called IL-6 transsignaling. In humans, sIL-6R is generated either by alternative splicing or by proteolytic release of the ectodomain of the membrane-bound IL-6R, whereas in the mouse, sIL-6R is exclusively generated by proteolysis (Rose-John and Heinrich, 1994). All of these events result in the dimerization of phosphorylated Stat3 monomers via Src homology-2 (SH2) domains, shifting them into a transcriptionally active conformation. Stat3 regulates its own endogenous inhibitor, Socs3, to form a negative feedback loop (Yu et al., 2009).

Stat3 activation in PDAC has been documented in human tissues and pancreatic cancer cell lines, although the mechanism of Stat3 activation in the absence of *JAK2* mutations and its function in pancreatic oncogenesis has not been examined (Kocher et al., 2007; Scholz et al., 2003).

In the present study, we aim to identify the role of the IL-6 dependent Stat3 signaling pathway in pancreatic cancer using genetically engineered mouse models.

RESULTS

Non-Cell-Autonomous Activation of Stat3^{Y705} in Pancreatic Cancer

Although Stat3 activation occurs in human PanIN, PC, and pancreatic cancer cell lines, its function in pancreatic carcinogenesis has not been examined (Scholz et al., 2003). First, we determined whether this finding could be repeated in *Kras*^{G12D} mice. *Kras*^{G12D} mouse lines express a constitutively active form of mutated K-Ras in the pancreas, thereby recapitulating the entire spectrum of pancreatic carcinogenesis that is observed in humans (Hingorani et al., 2003).

Phosphorylation of Stat3^{Y705} was analyzed in four PDACs (ID 14128, 9907, 17027, 16069) (see Table S1 available online) derived from *Kras*^{G12D} mice by immunohistochemistry (IHC) and immunoblot (IB). By IB, p-Stat3^{Y705} levels were highest in PDAC (ID 9907, 16069, 17027) compared with 18 week old non-tumor *Kras*^{G12D} mice, which harbor numerous low-grade PanIN lesions. Normal pancreas (LSL-*Kras*^{G12D}) was negative for p-Stat3^{Y705} (Figure 1A).

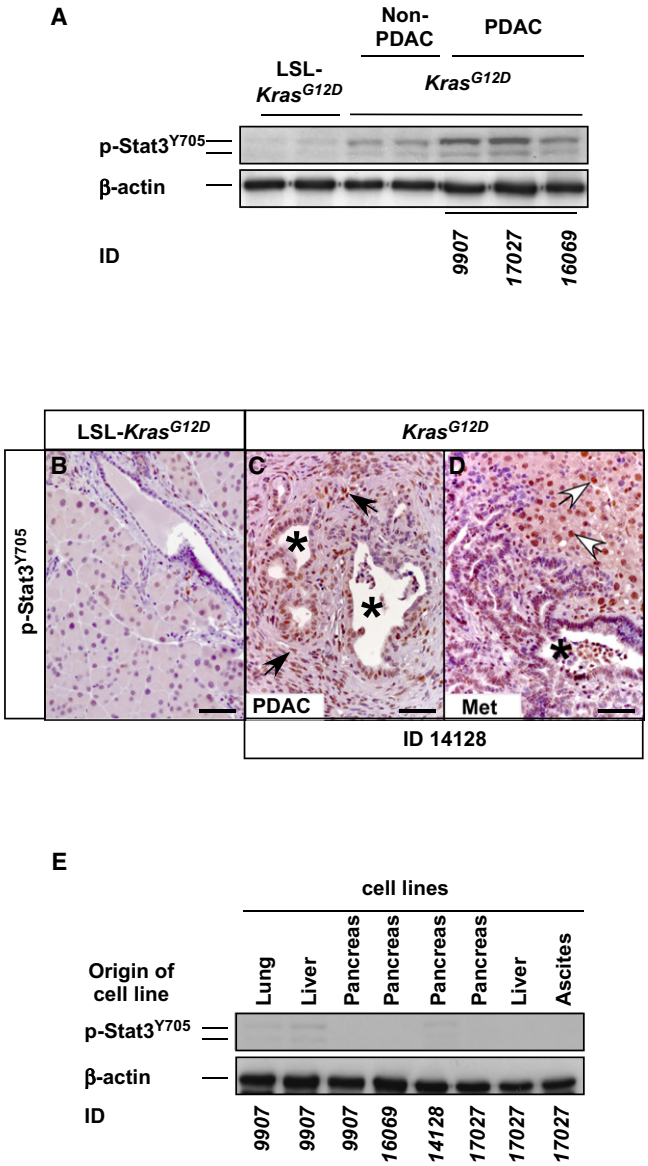

Figure 1. Non-Cell-Autonomous Activation of Stat3^{Y705} in Pancreatic Cancer

(A) Western blot analysis of p-Stat3^{Y705} in normal pancreas (LSL-*Kras*^{G12D}) and 18 week old noncancer-bearing *Kras*^{G12D} (non-PDAC) and cancer-bearing *Kras*^{G12D} (PDAC) (ID 9907, 16069, 17027) mice.

(B–D) Immunohistochemical analysis of p-Stat3^{Y705} in LSL-*Kras*^{G12D} pancreas (B), pancreatic cancer (C), and liver metastases (D) from *Kras*^{G12D} mice (representative PDAC, ID 14128). Black arrows indicate p-Stat3^{Y705} in infiltrating cells (C); white arrows indicate hepatocytes (D). Black stars indicate malignant cells.

(E) Various cell lines from primary tumors and metastases were examined for constitutive phosphorylation of Stat3. β-actin served as the control. Scale bars equal 50 μM.

See also Table S1.

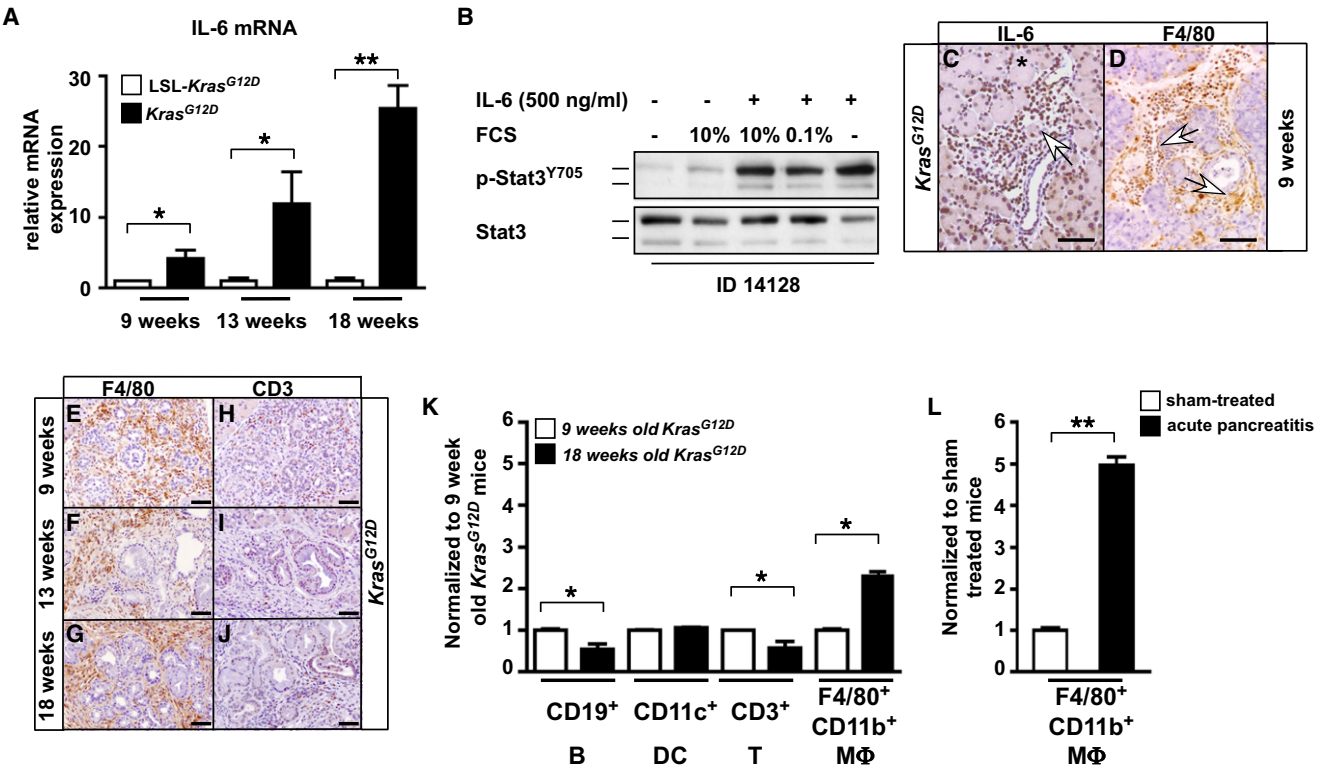

Figure 2. Myeloid Cells are the Cellular Source of IL-6

(A) Relative expression of IL-6 mRNA in whole pancreas in 9, 13, and 18 week old $Kras^{G12D}$ mice. Data are expressed as fold increase compared with controls (LSL- $Kras^{G12D}$ mice). Means ± SD ($n \geq 5$). *$p < 0.05$. **$p < 0.005$.

(B) IL-6-dependent activation of p-Stat3^{Y705} in one representative PDAC cell line (ID 14128).

(C and D) Immunohistochemical localization of F/80 and IL-6 in the pancreas of 9 week old $Kras^{G12D}$ mice. White arrows indicate infiltrating cells; black star indicates acini.

(E–J) Immunohistochemical staining of F4/80 and CD3 in the pancreas of 9, 13, and 18 week old $Kras^{G12D}$ mice.

(K) Pancreata from three mice were pooled and analyzed for macrophages ($CD45^+$ $F4/80^+CD11b^+CD11c^-$), dendritic cell ($CD45^+CD11c^+CD11b^+F4/80^-$), T cell ($CD45^+CD3^+$), and B cell ($CD45^+CD19^+$) content by fluorescence-activated cell sorting (FACS). The percentages of these cells were determined and normalized to 9 week old mice. Means ± SD ($n = 3$), *$p < 0.05$.

(L) Percentages of macrophages ($CD45^+F4/80^+CD11b^+CD11c^-$) in the pancreas during acute pancreatitis. Acute pancreatitis was induced by repetitive hourly injections of cerulein. Pancreata from three C57BL/6 mice were pooled and analyzed by FACS. Means ± SD ($n = 3$), **$p < 0.005$. Scale bars equal 50 μM.

See also Figure S1.

By IHC of PDAC (ID 14128) in $Kras^{G12D}$ mice, we observed strong phosphorylation of Stat3 at tyrosine residue 705 in primary cancers (Figure 1C) and their metastases (Figure 1D) in contrast to normal pancreas (LSL-$Kras^{G12D}$) (Figure 1B), similar to findings in humans. Notably, p-Stat3^{Y705} was restricted to malignant cells (Figure 1B, black stars) and infiltrating cells (Figure 1B, black arrows) or hepatocytes (Figure 1B, white arrows) that surrounded the metastasis. These data suggest that the level of Stat3 activation correlates with the progression of PanINs to PDAC. Moreover, Stat3^{Y705} phosphorylation is restricted to malignant cells and cells in the microenvironment.

To examine the mechanism of Stat3 activation in vitro, we generated cell lines from primary (pancreas) and metastatic (liver, lung, ascites) tumors (ID 9907, 16069, 17027; see Table S1). In contrast to their primary tumors or metastases, the isolated cancer cell lines showed low-level Stat3 activation in vitro or none at all (Figure 1E; for ID numbers, see Table S1). This observation is consistent with non-cell-autonomous phosphorylation of Stat3. Likely, Stat3 phosphorylation depends on the microenvironment of the PDAC.

To determine the mechanisms and factors through which Stat3 is phosphorylated in vivo, we measured the expression of gp130 ligands (IL-6, LIF, OSM, CNTF, IL-11) in the pancreas of $Kras^{G12D}$ mice, because these ligands activate the Stat3 cascade. Only IL-6 mRNA levels increased robustly and time dependently (Figure 2A); the levels of LIF, OSM, CNTF, and IL-11 remained unchanged or rose slightly (Figure S1A). The primary cancer cell lines that were derived from $Kras^{G12D}$ mice (ID 14128) responded to IL-6, experiencing strong phosphorylation of Stat3 (Figure 2B).

Due to its high expression in nontumor $Kras^{G12D}$ mice and its abilty to activate the Stat3 cascade in PDAC cell lines, we determined the cellular source of IL-6. By IHC, IL-6 was expressed predominantly by infiltrating immune cells (Figure 2C, white arrow); acinar cells expressed low levels (Figure 2C, black star). These pancreatic infiltrates in $Kras^{G12D}$ mice comprised

primarily F4/80-positive macrophages (Figures 2D and 2E–2G) and rare CD3-positive (Figures 2H–2J) cells. The inflammatory response in $Kras^{G12D}$ mice was accompanied by the elevated expression of MCP-1, MIP-2, KC, MIP-1α, IL-1β, and ICAM-1 mRNA (Figure S1B).

To characterize the cellular composition of these infiltrates, we digested the pancreas to immunophenotype the inflammatory cells. By flow cytometry, among CD45-positive cells in $Kras^{G12D}$ mice, the fraction of $F4/80^+CD11b^+$ (macrophages, $CD45^+F4/80^+CD11b^+CD11c^-$) cells increased, as did $CD11c^+$ cells (dendritic cells, $CD45^+CD11c^+CD11b^+F4/80^-$) to a lesser extent (Figure 2K). However, the accumulation of $F4/80^+CD11b^+$ cells (macrophages) was less compared with that in acute pancreatitis (AP) (Figure 2L). Consistent with the immunohistochemistry findings, the cellular proportion of lymphocytes did not increase.

In summary, our data demonstrate the time-dependent recruitment of inflammatory cells to the pancreas in $Kras^{G12D}$ mice. We identified macrophages ($CD45^+F4/80^+CD11b^+CD11c^-$) as the chief component of the cellular infiltrate and the source of IL-6 during pancreatic oncogenesis.

IL-6 Transsignaling Promotes PanIN Progression

Based on these findings, we hypothesized that Stat3 activation in pancreatic oncogenesis depends on the microenvironment, particularly on myeloid cells that secrete the gp130 ligand IL-6. To examine the interaction between macrophages and acinar cells that harbor $Kras^{G12D}$, we developed a coculture system in which macrophages were isolated from the pancreas of 18 week old $Kras^{G12D}$ mice and incubated with acinar cells derived from $Kras^{G12D}$ mice. Even prestimulation of the macrophages with IL-6 was insufficent to induce robust Stat3 activation in $Kras^{G12D}$ acinar cells. These data suggest that factors other than IL-6 are required to activate Stat3 in acinar cells from $Kras^{G12D}$ mice (Figure S2A).

IL-6 signals are transmitted via gp130 through IL-6 engagement of IL-6R or formation of a complex with soluble IL-6R, that latter of which is called IL-6 transsignaling. To determine the effects of IL-6 on the pancreas, we extended our in vitro analysis in acinar cells that were isolated from $Kras^{G12D}$ mice.

As shown in Figure 3A, only the IL-6R/IL-6 complex (termed as Hyper-IL-6) induced robust phosphorylation of Stat3 in acinar cells; IL-6 resulted only in slight phosphorylation. These data suggest that acinar cells require IL-6 transsignaling, rather than classical IL-6 signaling, to activate Stat3 in response to IL-6.

To characterize the impact of classical and IL-6 transsignaling on PanIN progression in vivo, $Kras^{G12D}$ mice were interbred with $Il\text{-}6^{-/-}$ and $sgp130^{tg}$ mice to obtain $Kras^{G12D};Il\text{-}6^{-/-}$ and $Kras^{G12D};sgp130^{tg}$ mice. Transgenic $sgp130^{tg}$ mice postnatally overexpress circulating sgp130Fc postnatally under control of the hepatic PEPCK promoter, thereby specifically inhibiting IL-6 transsignaling (Rabe et al., 2008). The genetic deletion of IL-6 in $Il\text{-}6^{-/-}$ mice occurs in the germ line and affects classical and IL-6 transsignaling. These strains were observed for 18 weeks.

By histology, $Kras^{G12D}$ mice developed numerous MUC5-positive (Figure 3D), low- and high-grade PanINs (Figures 3B and 3C, black arrow and black star) at 18 weeks, while $Kras^{G12D};Il\text{-}6^{-/-}$ mice had fewer and predominantly low-grade PanINs (Figures 3E–3G). Notably, postnatal inactivation of IL-6 transsignaling in $Kras^{G12D};sgp130^{tg}$ mice had a similar effect on PanIN formation: PanIN-1 and PanIN-2 lesion numbers fell significantly in these mice (Figures 3H–3K). Impaired PanIN progression correlated with phosphorylated Stat3 levels in the pancreas; IHC and IB analysis demonstrated less phosphorylated Stat3 on tyrosine 705 in $Kras^{G12D};Il\text{-}6^{-/-}$ and $Kras^{G12D};sgp130^{tg}$ mice compared with $Kras^{G12D}$ mice (Figures 3L–3O).

Similar results were observed in reciprocal bone marrow chimeras. Bone marrow from wild-type (WT) ($Il\text{-}6^{+/+}$) or $Il\text{-}6^{-/-}$ mice was introduced into irradiated $Kras^{G12D}$, according to the schedule in Figure S2B. As shown in Figure S2C, reconstitution of $Kras^{G12D}$ mice with IL-6-competent ($Il\text{-}6^{+/+}$) bone marrow ($BM\text{-}Il\text{-}6^{+/+}Kras^{G12D}$) induced PanIN progression, as evidenced by PanIN-3 lesions throughout the entire pancreas in three of the four transplanted mice. None of the $BM\text{-}Il\text{-}6^{-/-}Kras^{G12D}$ mice developed high-grade PanIN lesions (Figures S2D–S2G). Accordingly, Stat3 phosphorylation in PanIN lesions was attenuated in $BM\text{-}Il\text{-}6^{-/-}Kras^{G12D}$ mice (Figures S2H–S2I).

Collectively, these data suggest that myeloid cells use IL-6 transsignaling rather than classical IL-6 signaling to promote PanIN progression. The downstream effector Stat3 appears to be associated with the development of PanIN lesions.

Stat3 Constitutes a Central Node that Mediates PanIN Progression and PDAC Development

Because Stat3 is considered the major protumorigenic effector of IL-6, we determined the contribution of pancreatic Stat3 to PanIN progression and PC development. By immunofluorescence, we observed early phosphorylation of Stat3 at tyrosine residue 705 in the pancreas of 13-week-old $Kras^{G12D}$ mice (Figures 4A–4C, white star) and in infiltrating macrophages (Figures 4A–4C, white arrows). In parallel, the expression of *bona fide Stat3* target genes increased in the pancreas of these mice (data not shown). The widespread phosphorylation of Stat3 in the pancreas clearly suggested paracrine/autocrine stimulation rather than a cell-autonomous effect.

To examine the effect of Stat3 activation in the exocrine pancreas during oncogenesis, we generated compound mutant $Kras^{G12D}$ mice that lacked phosphorylatable $Stat3^{Y705}$ specifically in the exocrine pancreas and parts of the endocrine compartment using the $Ptf1a\text{-}cre^{ex1}$ mouse line ($Kras^{G12D};Stat3^{\Delta panc}$) (Algul et al., 2007a; Nakhai et al. 2007; Sano et al., 1999). *Stat3* inactivation had no effect on pancreatic development in adult mice, and basal proliferation rate and apoptotic index were indistinguishable between $Stat3^{\Delta panc}$ and $Stat3^{F/F}$ under steady-state conditions (to be published elsewhere).

Inactivation of the Stat3 pathway was confirmed by IB analysis. Whereas $Kras^{G12D}$ mice experienced strong Stat3 phosphorylation at tyrosine residue 705 at 9 and 13 weeks, *Stat3*-deficient $Kras^{G12D}$ mice failed to express p-$Stat3^{Y705}$. In contrast, Stat1 phosphorylation did not differ between genotypes (Figure 4D). Consistent with the $Kras^{G12D}$ expression in both mouse lines, total protein lysates from the pancreata of compound mutant mice expressed increased levels of activated and GTP-bound Ras (not significant between lines), concomitant with the induction of the downstream targets ERK1 and ERK2 (Figure 4E).

Notably, the typical macroscopic appearance (enlarged pancreas and focally nodular parenchyma) of $Kras^{G12D}$ mice was absent in $Kras^{G12D};Stat3^{\Delta panc}$ mice 13 weeks postpartum (p.p.); the $Kras^{G12D};Stat3^{\Delta panc}$ pancreas was similar to that in

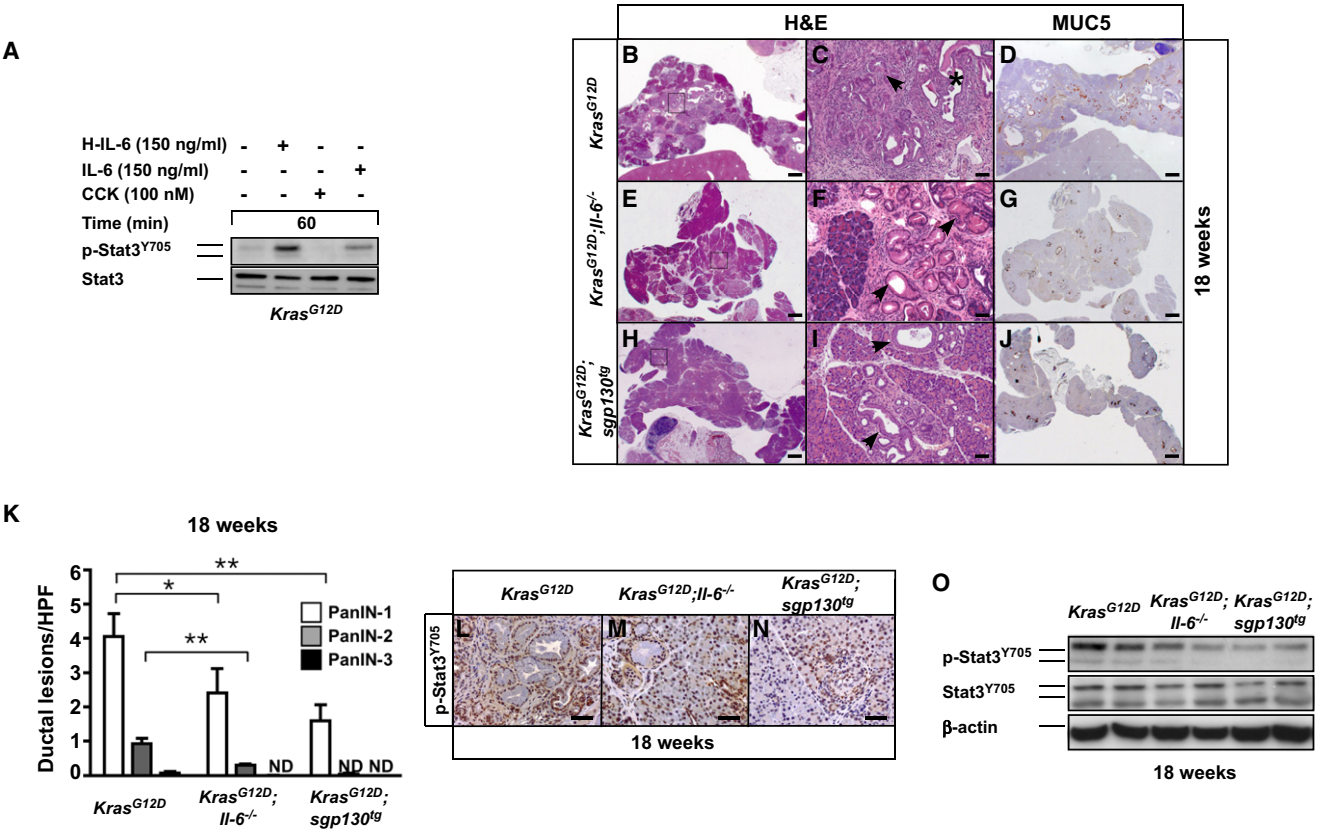

Figure 3. IL-6 Transsignaling Promotes PanIN Progression

(A) Stimulation of isolated acinar cells derived from *Kras*^{G12D} mice. Acinar cells were incubated with CCK (100 nM), IL-6 (150 ng/ml), or Hyper-IL-6 (H-IL-6 150 ng/ml) or were untreated. Lysates were analyzed for p-Stat3^{Y705}. Stat3 served as the positive control.

(B–J) Representative H&E-stained pancreatic sections from 18 week old *Kras*^{G12D} (B and C), *Kras*^{G12D};*Il-6*$^{-/-}$ (E and F), and *Kras*^{G12D};*sgp130*^{tg} mice (H and I). Black star indicates PanIN-3 lesions; black arrows indicate PanIN-1 lesions. Immunohistochemical analysis of MUC5 in the pancreas of 18 week old *Kras*^{G12D} (D) *Kras*^{G12D};*Il-6*$^{-/-}$ (G) and *Kras*^{G12D};*sgp130*^{tg} (J) mice.

(K) Number of PanINs was counted per 200x field. Means ± SD (n = 6), *p < 0.05 and **p < 0.005; ND, (not detectable).

(L–N) Immunohistochemical detection of p-Stat3^{Y705} in 18 week old mice of the indicated genotypes.

(O) Immunoblot analysis of p-Stat3^{Y705} and Stat3 in lysates from *Kras*^{G12D}, *Kras*^{G12D};*Il-6*$^{-/-}$, and *Kras*^{G12D};*sgp130*^{tg} mice.

Scale bars equal 500 μM (B, E, H, D, G, and J) and 50 μM (C, F, I, L, M, and N). See also Figure S2.

LSL-*Kras*^{G12D} mice (Figure 4F). Histologically, *Kras*^{G12D} mice developed progressive PanIN lesions (Figures 4G–4L, black arrow), which was not observed in *Kras*^{G12D};*Stat3*$^{\Delta panc}$ mice (Figures 4M–4R). Only rare reactive ducts (Figure 4P, white arrow) and low-grade PanIN lesions (PanIN-1) (Figure 4R, black arrow) were detectable in 13 and 18 week old mice, suggesting that *Stat3* inactivation in the pancreas prevents PanIN progression but not its initiation (Figure 4S).

To determine whether Stat3 inactivation influences PDAC development, we followed two cohorts, 20 *Kras*^{G12D} and 41 *Kras*^{G12D};*Stat3*$^{\Delta panc}$ mice, for nearly two years (Table 1; Table S1). The mice were sacrificed when they became moribund, particularly if they presented with weight loss, ascites, jaundice, a palpable abdominal mass, or any other compromising disease.

Only 24.5% (10/41) of the *Kras*^{G12D};*Stat3*$^{\Delta panc}$ mice developed PC, and 55% (11/20) of *Kras*^{G12D} mice succumbed to PC (Figure 4T). Tumor proliferation index was significantly lower in Stat3-deficient *Kras*^{G12D} mice compared with *Kras*^{G12D} animals (Figure 4U). Tumors from *Kras*^{G12D};*Stat3*$^{\Delta panc}$ mice did not express nuclear Stat3 in the primary cancer or its metastasis (Figures S3A and S3B); in adjacent tissues, p-Stat3^{Y705} expression was restricted to inflammatory cells (Figure S3C). Accordingly, cell lines from *Kras*^{G12D};*Stat3*$^{\Delta panc}$ mice did not respond to IL-6 (Figure S3D) because they failed to phosphorylate Stat3.

Consequently, proliferation was delayed after incubation with various concentrations of FCS (Figure S3E) and IL-6 (Figures S3F). Similar results were obtained when these cell lines were incubated with Hyper-IL-6 (data not shown). These cell lines expressed a slightly smaller version of Stat3, termed as Stat3$^{\Delta panc}$.

Collectively, our data suggest that epithelial Stat3 is required for the transduction of tumor-promoting signals of IL-6, particularly during the progression of PanIN to PDAC, but not in the initiation of PanIN.

Stat3 Regulates Cell-Autnomous Effects during Pancreatic Oncogenesis in *Kras*^{G12D} Mice

Apoptosis is a rare event in early and late PanIN lesions, while proliferation is detectable and predominant throughout progression (Luttges et al., 2003). Thus, we analyzed these aspects to determine the molecular mechanisms by which Stat3 confers

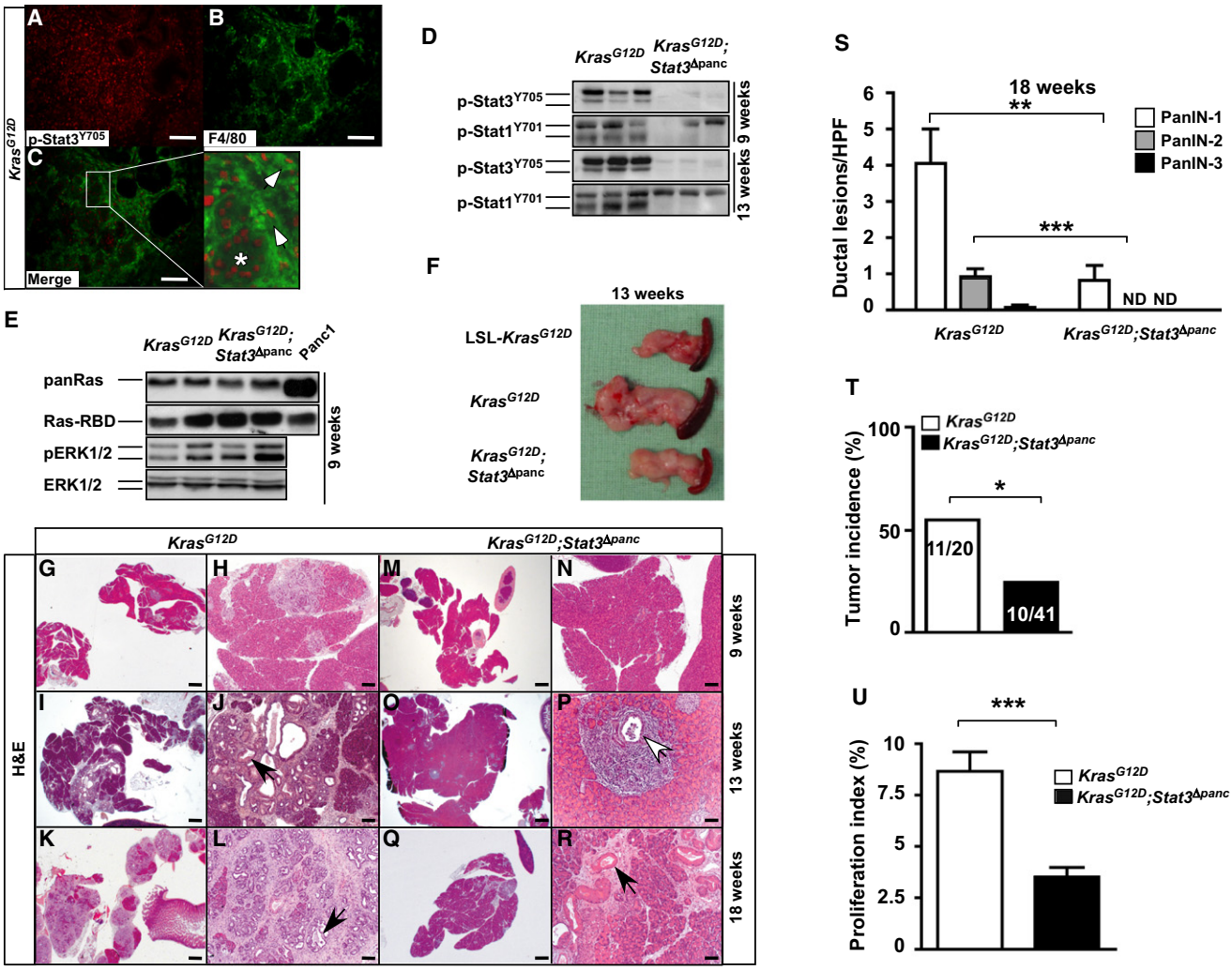

Figure 4. Stat3 Is Essential for PanIN Progression

(A–C) Immunofluorescence analysis of p-Stat3^{Y705} and F4/80 in pancreata of 13 week old LSL-*Kras*^{G12D} mice. White arrows indicate F4/80-positive macrophages, white star acini (see magnification).

(D) Immunoblot analysis of p-Stat3^{Y705} and p-Stat1^{Y701} in lysates from *Kras*^{G12D} and *Kras*^{G12D};*Stat3*$^{\Delta panc}$ mice.

(E) Immunoprecipitation of activated Ras with Raf-1 RBD agarose. Immunoblot analysis with anti-Ras and p-ERK1/2 and ERK1/2. Panc-1 lysates were positive controls.

(F) Macroscopic view of pancreas from LSL-*Kras*^{G12D}, *Kras*^{G12D}, and *Kras*^{G12D};*Stat3*$^{\Delta panc}$ mice.

(G–R) Representative H&E-stained sections from mice of the indicated genotypes. Black arrows indicate PanIN lesions; white arrow is reactive ducts.

(S) Number of PanINs was counted per 200x field. Means ± SD (n = 6), **p < 0.005, ***p < 0.0005. ND, not detectable.

(T) Determination of tumor incidence in both mouse cohorts, *p < 0.05.

(U) Proliferation index was measured in BrdU-stained PC sections from *Kras*^{G12D} (n = 9) and *Kras*^{G12D};*Stat3*$^{\Delta panc}$ mice. Means ± SD (n = 5), ***p < 0.0005. Scale bars equal 50 μM (A, B, C, H, J, L, N, P, and R) and 500 μM (G, I, K, M, O, and Q). See also Figure S3.

its tumorigenic properties. To examine whether pancreas-specific inactivation of the Stat3 cascade renders acinar/ductal cells more susceptible to apoptosis, we measured caspase-3 cleavage in 13 week old mice by IHC.

Many acinar and ductal cells in the pancreas of *Kras*^{G12D};*Stat3*$^{\Delta panc}$ mice were positive for cleaved caspase-3 (Figure 5A, magnified box), which was absent in *Kras*^{G12D} mice (Figure 5B, magnified box); this finding was confirmed by quantification (Figure 5C) and immunoblot analysis (data not shown). By immunoblot, Bcl-X_L, Survivin, and Mcl-1 were upregulated in *Kras*^{G12D} mice but absent in *Kras*^{G12D};*Stat3*$^{\Delta panc}$ mice, consistent with findings that *bcl-x*, *survivin,* and *mcl-1* are transcriptionally induced by Stat3 (Figure S4A) (Yu et al., 2009).

To determine whether Stat3 regulates proliferation in the pancreas of *Kras*^{G12D} mice, we injected mice with 5-bromo-2-deoxyuridine (BrdU), which incorporates into newly synthesized DNA, and sacrificed the animals two hours later. By anti-BrdU staining, we observed the time-dependent incorporation of BrdU into acinar and ductal cells (data not shown), but mice that were deficient for phosphorylable Stat3^{Y705} expressed fewer BrdU-positive cells in the pancreas, even after 13 weeks of age (Figure 5D). Consistent with this result, proliferating cell

Table 1. Clinical Spectrum of Diseases in *Kras^{G12D};Stat3$^{\Delta panc}$* Mice

ID	Age (days)	PDAC	Histology	Liver	Lung	Diaphragm	Ascites	Other
302	369	Y	G	Y^M	Y^M	N	N	BO, pLN
303	240	N		N	N	N	N	A
317	480	N		N	N	N	N	A
320	426	N		N	N	N	N	A
321	484	Y	U	Y^M	N	N	N	P
322	537	N		N	N	N	N	A
352	445	Y	U	Y^M	Y^M	Y^M	N	pLN
362	329	Y	G	Y^M	Y^M	N	N	BO
365	381	Y	G	N	N	N	Y	
370	314	N		N	N	N	N	SD
371	213	N		N	N	N	N	
407	361	Y	U	N	N	N	N	P
408	396	N		N	N	N	N	A
419	445	Y	U	N	N	N	N	
2163	413	Y	U	Y^M	N	N	Y	pLN, BO
2206	113	N		N	N	N	N	SD
2755	331	N		N	N	N	N	A, SD
2756	239	N		N	N	N	N	
2827	213	N		N	N	N	N	P
2865	489	N		N	N	N	N	A
2950	573	N		N	N	N	N	A
2951	438	N		N	N	N	N	A
2959	306	N		N	N	N	N	A
2969	386	N		N	N	N	N	A, SD
2992	136	Y	G	N	N	N	N	
3038	707	N		N	N	N	N	A, SD
3045	447	N		N	N	N	N	P
3050	699	N		N	N	N	N	A
3098	166	N		N	N	N	N	A
3103	426	N		N	N	N	N	A
3140	683	N		N	N	N	N	A
3141	418	N		N	N	N	N	A
3142	510	N		N	N	N	N	A
3144	320	N		N	N	N	N	A, P
5101	609	N		N	N	N	N	
5105	609	N		N	N	N	N	
5110	277	N		N	N	N	N	A, SD
5185	191	Y	G	N	N	N	N	SD
5277	341	N		N	N	N	N	A, SD
5311	233	N		N	N	N	N	A
5530	452	N		N	N	N	N	A
Totals		10/41		5/41	3/41	1/41	2/41	

pLN, peripancreatic lymph node; M, metastasis; pC, pancreatic cyst; U, undifferentiated; G, glandular; A, atrophy; SD, skin disease; BO, biliary obstruction; P, paralysis.

nuclear antigen (PCNA) expression was generally higher in *Kras^{G12D}* mice (Figure 5E).

Next, we identified proteins that were expressed during proliferation by generating pancreatic protein lysates from 9 and 13 week old *Kras^{G12D}* and *Kras^{G12D};Stat3$^{\Delta panc}$* mice and performing immunoblot analysis of cell cycle regulators. The time-dependent induction of Cyclin D1 and c-myc was attenuated in *Kras^{G12D};Stat3$^{\Delta panc}$* mice, suggesting that Stat3^{Y705} phosphorylation regulates proliferation during *Kras^{G12D}*-driven PanIN progression (Figure 5E).

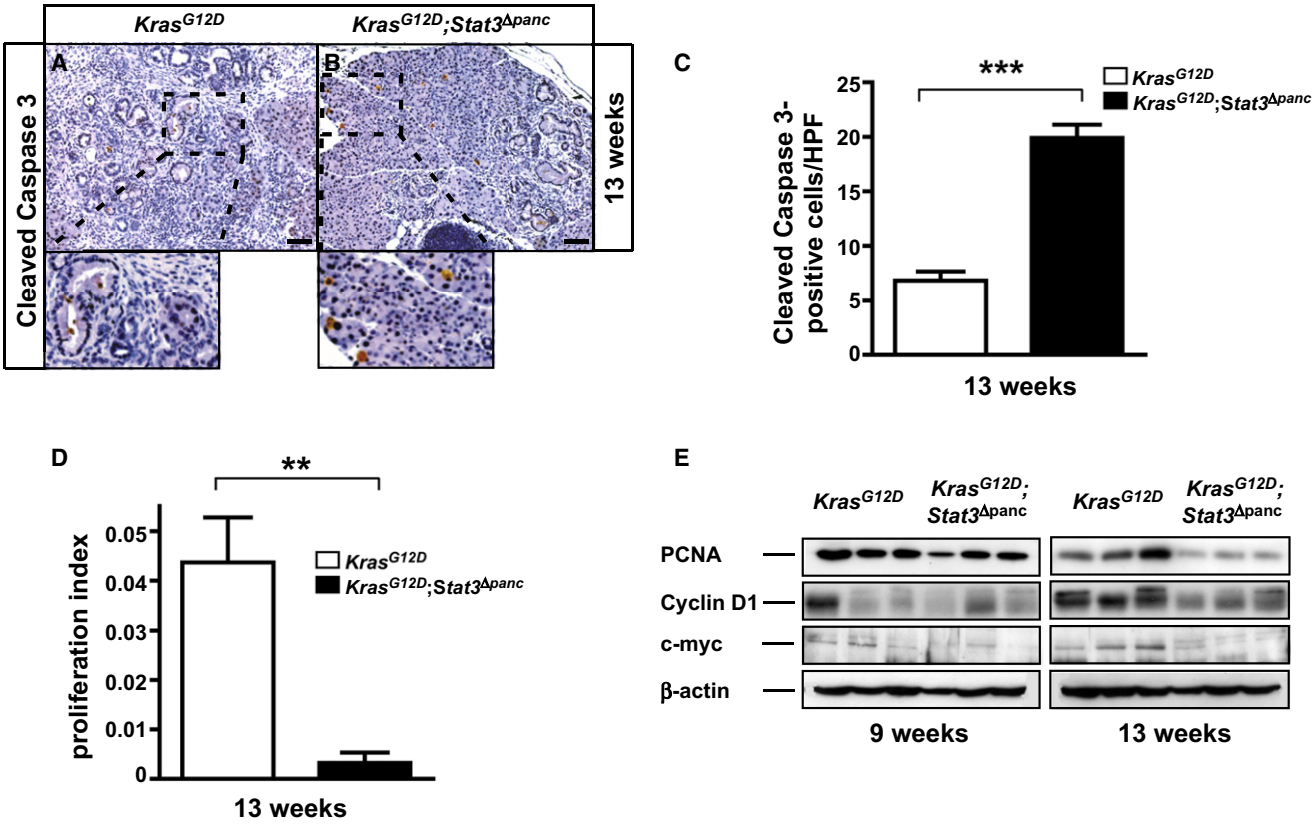

Figure 5. Stat3 Regulates Apoptosis and Influences Cell Cycle Progression during PanIN Progression

(A and B) Immunohistochemical analysis of cleaved caspase-3 in pancreata of $Kras^{G12D}$ and $Kras^{G12D};Stat3^{\Delta panc}$ mice.

(C) Apoptosis (cleaved caspase-3) index in pancreas of $Kras^{G12D}$ (n = 6 mice, 20 fields per mouse) and $Kras^{G12D};Stat3^{\Delta panc}$ mice (n = 7 mice, 20 fields per mouse). Means ± SD, ***p < 0.0005.

(D) BrdU proliferation index of pancreas in $Kras^{G12D}$ (n = 6 mice, 20 fields per mouse) and $Kras^{G12D};Stat3^{\Delta panc}$ mice (n = 7 mice, 20 fields per mouse). Means ± SD ($n \geq 5$), **p < 0.005.

(E) Immunoblot analysis of the indicated proteins in lysates from both genotypes. Scale bars equal 200 μM.

See also Figure S4.

Further, Stat3 seems to be involved in concomitant inflammation in the pancreas, as the accumulation of F4/80-positive macrophages declined in Stat3-proficient mice (Figures S4B and S4C). In addition, the Stat3-dependent and proinflammatory enzyme Cox-2 was not expressed in $Kras^{G12D};Stat3^{\Delta panc}$ mice compared with $Kras^{G12D}$ animals (Figure S4D). Cox-2 was detectable in acinar cells and in ductal lesions (Figures S4E and S4F).

Based on our data, we conclude that Stat3 activation regulates $Kras^{G12D}$-dependent effects on apoptosis, proliferation, and inflammation.

Homozygous Deletion of *Socs3* Accelerates PanIN Progression and Promotes PDAC Development

Although Stat3 regulates PanIN progression, it is unknown whether Stat3 alone is sufficient to mediate these effects. Stat3 activation is tightly regulated by the endogenous feedback inhibitor Socs3, which inhibits Stat3 signaling by binding to gp130.

$Kras^{G12D}$ mice expressed high levels of *Socs3* mRNA (Figure 6A). Socs3 was detectable in acinar cells (Figure 6B, black arrows) and PanIN lesions (Figure 6B, white arrows) of $Kras^{G12D}$ mice.

To induce early and prolonged activation of p-Stat3^{Y705} in the pancreas of these mice, we generated a mutant mouse line that lacked *Socs3* specifically in the pancreas (Nakaya et al., 2009). Hetero- or homozygous deletion of *Socs3* did not affect pancreatic morphology or cellular homeostasis (data not shown). Homozygous deletion of *Socs3* in $Kras^{G12D}$ mice ($Kras^{G12D};Socs3^{\Delta panc}$), however, induced early and high phosphorylation levels of Stat3^{Y705} in the pancreas as early as four weeks of age (Figure 6C).

At this age, $Kras^{G12D};Socs3^{\Delta panc}$ mice developed large areas of reactive ducts (Figure 6K) and low- (Figure 6H) and high-grade (Figure 6E) PanINs throughout the pancreas (Figure 6D). The nuclei of ductal lesions and acinar cells were positive for phosphorylated Stat3^{Y705} (Figures 6F–6L) and Cyclin D1 (Figures 6G–6M). By quantification of ductal lesions, we observed rapid progression of PanINs in these mice (Figure 6N).

To determine whether the deletion of Socs3 and the subsequent early and robust activation of Stat3 influences PDAC development, we monitored 41 $Kras^{G12D};Socs3^{\Delta panc}$ mice for

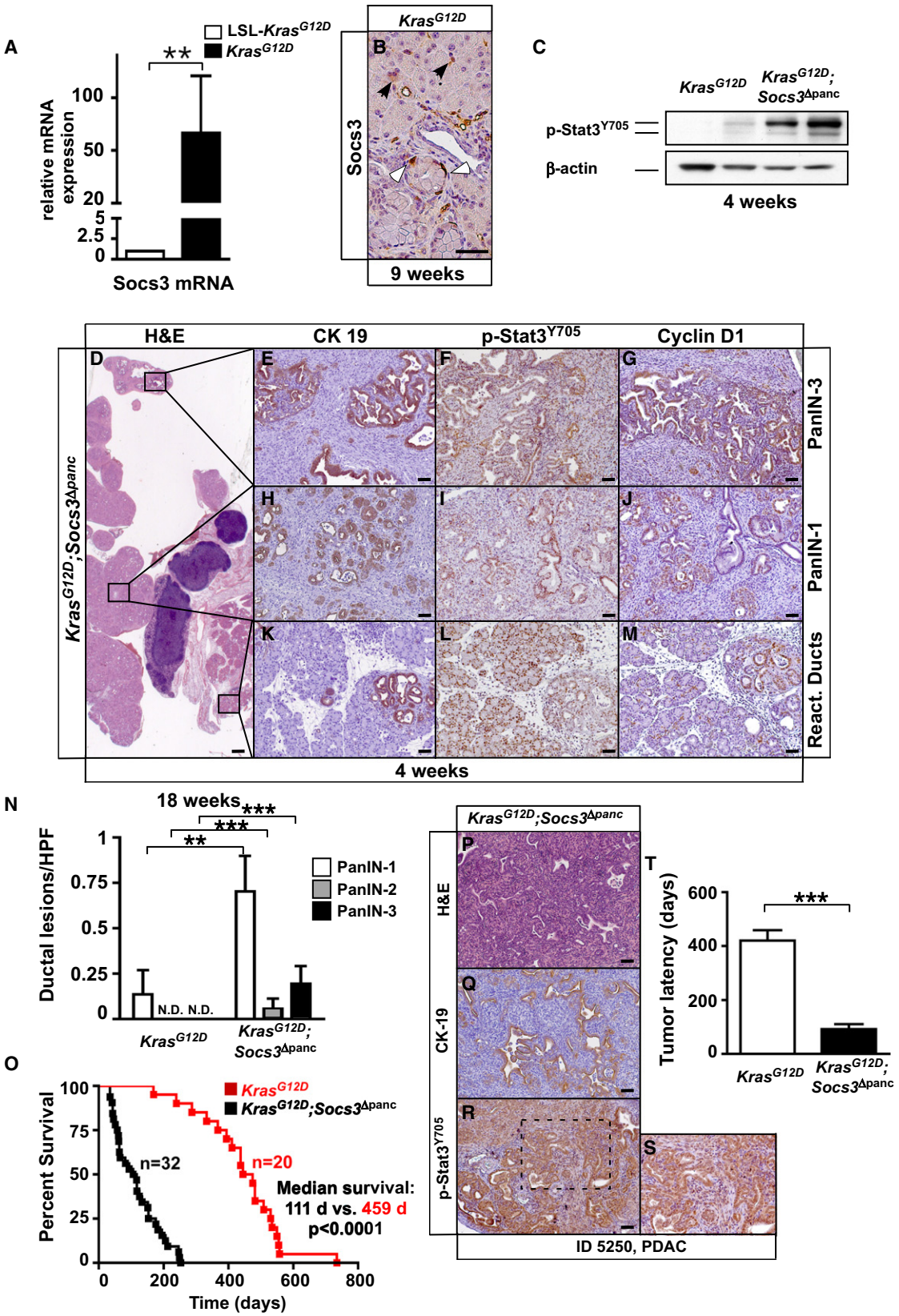
A
LSL-KrasG12D
KrasG12D
**
relative mRNA expression
100
50
20
5
2.5
0
Socs3 mRNA
KrasG12D
B
Socs3
9 weeks
C
KrasG12D
KrasG12D; Socs3Δpanc
p-Stat3Y705
β-actin
4 weeks
H&E
CK 19
p-Stat3Y705
Cyclin D1
D
E
F
G
H
I
J
K
L
M
KrasG12D;Socs3Δpanc
PanIN-3
PanIN-1
React. Ducts
4 weeks
N
18 weeks
***
***
**
Ductal lesions/HPF
1
0.75
0.5
0.25
0
PanIN-1
PanIN-2
PanIN-3
N.D. N.D.
KrasG12D
KrasG12D; Socs3Δpanc
O
Percent Survival
100
75
50
25
0
KrasG12D
KrasG12D;Socs3Δpanc
n=32
n=20
Median survival:
111 d vs. 459 d
p<0.0001
0
200
400
600
800
Time (days)
KrasG12D;Socs3Δpanc
P
H&E
Q
CK-19
R
p-Stat3Y705
S
ID 5250, PDAC
T
Tumor latency (days)
600
400
200
0
***
KrasG12D
KrasG12D; Socs3Δpanc

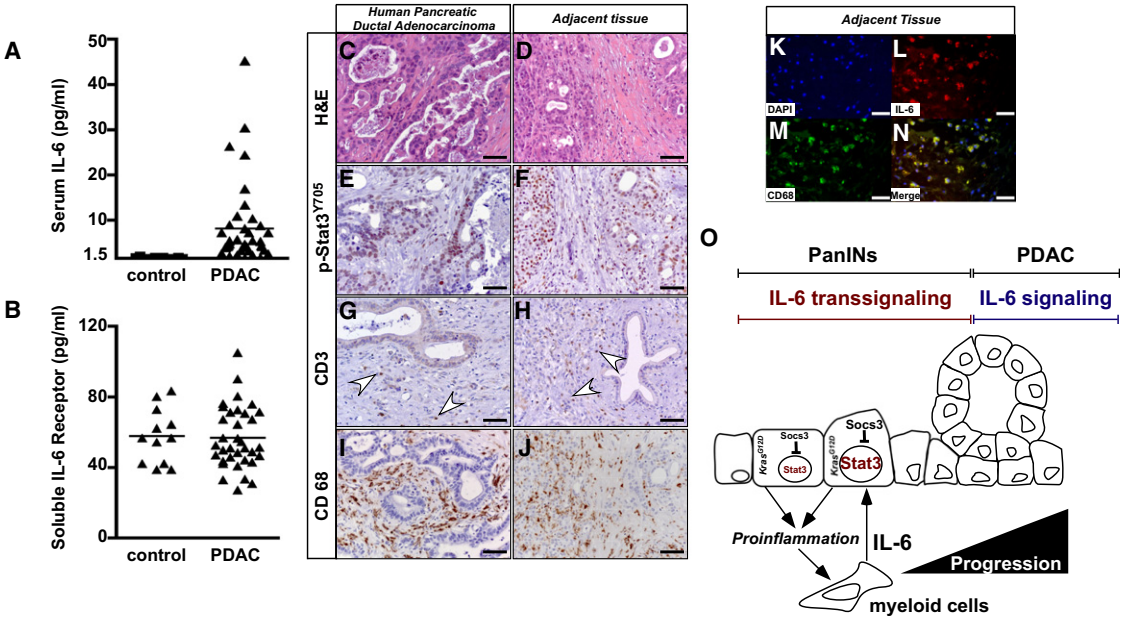

Figure 7. Evidence of IL-6/Stat3 Cascade in Human PDAC

(A and B) Analysis of IL-6 and soluble IL-6R in patients with PDAC.

(C–J) H&E staining and detection of p-Stat3^{Y705}, CD3, and CD68 in human PDAC (B–E) and in adjacent nonmalignant tissue (F–I). White arrows indicate infiltrating cells.

(K–N) Immunofluorescence analysis of human specimens. Nuclei were visualized with DAPI. Anti-IL-6 and anti-CD68 were used to label IL-6 and macrophages. Signals were merged to identify the site of IL-6 production.

(O) Scheme of the central role of Stat3 in PanIN progression and PDAC development. Scale bars equal 50 μM.

nearly one year (Table S2). The combination of activated *Kras*^{G12D} and Socs3 deficiency led to significant decreases in body and pancreatic weight (data not shown). As shown in Figure 6O, these mice reached terminal morbidity between 6 and 31 weeks of age and had a median survival of 111 days ($p < 0.0001$ for *Kras*^{G12D};*Socs3*$^{\Delta panc}$ colony compared with *Kras*^{G12D} cohort). Within the observation period, 37.5% (12/32) of *Kras*^{G12D};*Socs3*$^{\Delta panc}$ mice developed pancreatic cancer (Table S2). These ductal adenocarcinomas (Figure 6P) were positive for CK-19 (Figure 6Q) and p-Stat3^{Y705} (Figure 6R). Phosphorylated Stat3^{Y705} was restricted primarily to the nuclei of cancer cells (Figure 6S). Tumor latency in these mice was lower compared with *Kras*^{G12D} mice (93 vs 428 days, Figure 6T).

Collectively, these results suggest that levels of Stat3 phosphorylation determine the progression of PanIN lesions to pancreatic cancer.

Evidence for the IL-6/Stat3 Cascade in Human PDAC

To determine the relevance of the observed link between myeloid IL-6 and p-Stat3^{Y705} in PDAC, we measured IL-6 and soluble IL-6-receptor (sIL-6R) levels in patients with PDAC. Serum IL-6 levels in 39 patients were significantly higher than in healthy control groups (Figure 7A), and sIL-6R levels did not differ (Figure 7B).

Based on the the significantly high systemic levels of IL-6 and the presence of sIL-6R in patients, we examined whether the IL-6/Stat3 cascade was detectable locally in human specimens (Figures 7C and 7D) by performing the IHC of p-Stat3^{Y705} and IL-6 in human specimens of PDAC. Notably, Stat3 was activated in PDAC (Figure 7E) and in the acinar cells or early PanIN lesions in tumor-adjacent tissues, similar to the observations in our mouse models (Figure 7F). Most infiltrating cells were macrophages by anti-CD68 staining (Figure 7E), and CD3-positive

Figure 6. Homozygous Deletion of *Socs3* Enhances Stat3 Activation, Promotes PDAC Development, and Reduces Survival in Kras^{G12D} Mice

(A) Relative expression of Socs3 mRNA in pancreas from 9 week old *Kras*^{G12D} mice. Means ± SD ($n \geq 5$), $^{**}p < 0.005$.

(B) Immunohistochemical localization of Socs3 in the pancreas of 9 week old *Kras*^{G12D} mice. Black arrows indicate positivity within acini, white arrows positivity within PanIN lesions.

(C) Immunoblot analysis of p-Stat3^{Y705} and β-actin in lysates from 4 week old *Kras*^{G12D} and *Kras*^{G12D};*Socs3*$^{\Delta panc}$ mice.

(D–M) Representative H&E staining and detection of CK-19, p-Stat3^{Y705}, and Cyclin D1 in pancreas from 4 week old *Kras*^{G12D};*Socs3*$^{\Delta panc}$ mice.

(N) Number of PanINs was counted per 200x field. Means ± SD ($n = 5$), $^{**}p < 0.005$, and $^{***}p < 0.0005$. ND, (not detectable).

(O) Kaplan-Meier curves show a median survival in *Kras*^{G12D};*Socs3*$^{\Delta panc}$ mice of 111 days, significantly less (459 days) than *Kras*^{G12D} mice ($p < 0.0001$, log-rank test, for pairwise combination).

(P–S) Ductal adenocarcinoma (P) from an approximately 2 month old mouse (ID 5250), demonstrating CK-19 (Q) expression and abundant nuclear localization of p-Stat3^{Y705} (R, see magnification in S).

(T) Tumor latency in *Kras*^{G12D} ($n = 11$) and *Kras*^{G12D};*Socs3*$^{\Delta panc}$ ($n = 12$) cohorts. Means ± SD, $^{***}p < 0.0005$.

Scale bars equal 500 μM (D) and 50 μM (B, E–M, and P–R). See also Table S2.

lymphocytes were scattered around cancer cell clusters and preneoplastic lesions (Figures 7G and 7H). In tumor-adjacent tissues, macrophages were observed between nontransformed acini (Figure 7I). By immunofluorescence, macrophages were determined to be the principal source of IL-6 (Figures 7K–7N).

Collectively, these data suggest that the basis for classical IL-6 and IL-6 transsignaling, linking myeloid IL-6 to p-Stat3^{Y705} in preneoplastic or neoplastic cells, exists in human PDAC and potentially define a mechanism of pancreatic oncogenesis.

DISCUSSION

Aberrant activation of Stat3 in the absence of Jak2 mutations is a recurring theme in human PDAC; however, its implication in pancreatic oncogenesis in vivo has remained undetermined (Glienke et al., 2010; Hutzen et al., 2009; Lin et al., 2010b; Scholz et al., 2003). Using genetic and pharmacological tools, we identified important functions of IL-6 and Stat3 and their implications for multiple aspects of pancreatic oncogenesis.

Also, we detailed a signaling network between stromal and preneoplastic pancreatic cells and identified Stat3 as the critical node in this interplay. Our study provides evidence that myeloid cells release IL-6 to induce Stat3 activation in the pancreas via IL-6 transsignaling, thus potentiating a feed-forward response in the tumor microenvironment to promote PanIN progression and, ultimately, PDAC development in vivo. Genetic inactivation of classical IL-6 signaling, IL-6 transsignaling, and the Stat3 effector pathway impaired PanIN progression and PDAC development (Figure 7O).

By identifying the underlying mechanisms, we have explained the implications of IL-6 and myeloid cells in human PDAC mechanistically. Many studies have observed a robust and consistent assocation of IL-6 with patient outcomes (Ebrahimi et al., 2004; Talar-Wojnarowska et al., 2009), and a specific polymorphism of IL-6 has been reported to be overrepresented in such patients (Talar-Wojnarowska et al., 2009). The density of inflammatory cells in pancreatic carcinoma, especially of macrophages, has predictive value for patient prognoses (Kurahara et al., 2009).

In this study, we found that pancreatic myeloid cells mediate tumor promotion substantially by releasing IL-6 into the stroma. Consistent with this observation, enhanced pancreatic inflammation in *Kras*^{G12D} mice through repetitive application of the hormone cerulein accelerates PanIN progression and PDAC development, underscoring the significance of inflammatory cells in these settings (Guerra et al., 2007). Because cerulein fails to induce phosphorylation of Stat3 in acinar cells derived from *Kras*^{G12D} mice in vitro, we assume that inflammatory cells release IL-6 to induce p-Stat3 in the pancreas, thus promoting oncogenesis in this inflammation-associated model of PDAC.

The paracrine effects of IL-6, however, are not restricted to preneoplastic and cancer cells in the pancreas. We observed Stat3 activation in infiltrating macrophages and normal hepatocytes that surrounded metastatic lesions, suggesting a general effect of IL-6 on the various cells that constitute the microenvironment; whether this activation in nontransformed cells impacts oncogenesis or the formation of metastatic lesions is unknown.

The IL-6/Stat3 cascade appears to be ubiquitous—not restricted solely to the pancreas. In a model of inflammation-associated colorectal carcinogenesis, for example, myeloid IL-6 activates Stat3 to promote the formation of adenoma and tumors (Bollrath et al., 2009; Grivennikov et al., 2009). Our data do not exclude the involvement of other cytokines, because transgenic overexpression of *Il-1beta* in the pancreas has been shown to be sufficent to induce proliferation, robust desmoplasia, and rare acinar-ductal metaplasia (Marrache et al., 2008). Notably, IL-1β failed to acitvate Stat3 in pancreatic cancer cells, suggesting that other signaling pathways transmit its signals in the pancreas.

Although the involvement of IL-6 in cancer-promoting inflammation in various organs is well established, no study has implicated IL-6 or IL-6 transsignaling in spontaneous tumor formation. Using the *Kras*^{G12D} model in the pancreas, we defined a central function for IL-6 during oncogenesis.

Two distinct processes control IL-6 responses in vivo. IL-6 signals are transmitted via gp130 through IL-6 engagement of IL-6R or formation of a complex with soluble IL-6R (i.e., IL-6 transsignaling). Because IL-6R is sparsely expressed, IL-6 transsignaling increases the number of potential IL-6 target cells (Rose-John et al., 2006). Nontransformed acinar cells that express oncogenic *Kras*^{G12D} require IL-6 transsignaling to induce robust phosphorylation of Stat3. IL-6 itself is predominantly secreted by inflammatory cells, most likely in an NF-κB-dependent manner. Similarily, recruitment of these cells to the pancreas also involves induction of NF-κB, potentially as a consequence of *Kras*^{G12D} dependent activation (Finco et al., 1997). Beyond its capacity to secret IL-6, immune cells have also been shown to participate in the process of IL-6R shedding (Chalaris et al., 2007), a process that also involves the metalloproteinases ADAM17 (**a** **d**esintegrin **a**nd **m**etalloproteinase), and to a lesser extent ADAM10 (Matthews et al., 2003). In addition to its function as an important regulator of proinflammatory chemokines and cytokines, NF-κB might therefore be implicated in establishing IL-6 transsginaling during pancreatic oncogenesis (Algul et al., 2007c; Guerra et al., 2007). Whether the metallproteinases ADAM17 and ADAM10 has a role to play, and what role it plays, during pancreatic oncogenesis remains to be elucidated in further studies. Using genetic tools, we herein found that IL-6 transsignaling, not classical IL-6 signaling, entails Stat3 activation to promote PanIN progression in vivo. Thereby, our data extend previous findings implicating immune cells to include myeloid-derived suppressor cells, tumor-associated macrophages, and Treg in PDAC development (Clark et al., 2007).

The major protumorigenic IL-6 effector is Stat3, the ablation or prolonged activation in the pancreas of which influences PanIN progression but not PanIN initiation. Stat3 has been implicated in apoptosis and cell cycle progression during oncogenic (*Kras*^{G12D}) stress. We identified Stat3 activation as the chief mediator of programmed cell death. Stat3 upregulated the anti-apoptotic proteins Bcl-X_L, Mcl-1, and Survivin, which were recently demonstrated to be Stat3 target genes (Yu et al., 2009). Their activity during apoptosis in pancreatic cancer has also been observed.

Inhibition of Stat3 in human pancreatic cancer cells facilitates apoptosis and inhibits chemoresistance (Lin et al. 2010a). Persistent Stat3 activation during PanIN progression also mediates the proliferation of preneoplastic lesions in the pancreas.

Similarily, deletion of IKK in hepatocytes effects chronic Stat3 activation, inducing proliferation and promoting hepatocellular carcinoma on exposure to diethylnitrosamine (He et al., 2010). Consistent with this observation, Stat3 inactivation mitigates the incorporation of BrdU in the pancreas, paralleled by impaired induction of Cyclin D1 (Masuda et al., 2002) and c-myc (Barre et al., 2005), which are regulated by nuclear Stat3 and overexpressed in human specimens of PDAC (Kawesha et al., 2000). These factors are central in driving cancer cells from G0/G1 to S phase, propelling cell cycle progression. Similarly, isolated pancreatic cancer cell lines from Stat3-deficient $Kras^{G12D}$ mice proliferated less in response to FCS, IL-6, and Hyper-IL-6.

Intracellular regulation of Stat3 activation is tightly controlled by the concomitant expression of its endogenous inhibitor, Socs3 (Yu et al., 2009). In $Kras^{G12D}$ mice, we noted high pancreatic levels of Socs3, suggesting that the activation and inhibition of Stat3 are balanced during PanIN progression. Deleting both alleles of *Socs3* in $Kras^{G12D}$ tipped this balance toward robust phosphorylation of Stat3, which accelerated the progression of PanIN lesions and the development of PC. Survival and tumor latency were curtailed in Socs3-deficient $Kras^{G12D}$ mice. Thus, we propose that the Stat3/Socs3 pathway assumes a central role during pancreatic oncogenesis.

The most notable observations pertained to tumor cells from PDAC in $Kras^{G12D}$ mice. All cancer cell lines that we examined failed to exhibit constitutive phosphorlyation of Stat3, which formed the basis for our hypothesis that Stat3 activation during pancreatic oncogenesis depends on the microenvironment. These findings contrast other studies that have observed constitutive phosphorylation of Stat3 in nearly all human pancreatic cancer cell lines (Glienke et al. 2010; Greten et al., 2002; Hutzen et al., 2009; Kim et al. 2010; Lin et al. 2010a; Scholz et al., 2003; Trevino et al., 2006).

One explanation for this discrepancy proposes that additional mutations in p53 in human cancer cell lines mediate constitutive phosphorylation of Stat3, as seen in other tumor cells (Lin et al., 2002). Wild-type p53 regulates Stat3 phosphorylation in ovarian cancer cell lines (Caov-3 and MDAH2774) by controlling Jak2 through p53-dependent upregulation of protein tyrosine phosphatase 1-B (PTP-1B), which inactivates Jak2 (Reid et al., 2004). The balance between PTP-1B and Jak2 is likely to be dysregulated in human pancreatic cancer cell lines, because nearly all established human PDAC cell lines harbour p53 mutations (Sipos et al., 2003). In contrast, such mutations were absent in the cell lines that were derived from $Kras^{G12D}$ mice (data not shown).

We have identified an important mechanism that determines the progression and development of PanIN to PDAC. $Kras^{G12D}$-induced pancreatic oncogenesis depends on the microenvironment, wherein myeloid cells in the pancreas accelerate PanIN progression and PDAC development by releasing IL-6. In examining the routes of IL-6 dependent activation of Stat3, we have demonstrated a relevant function of IL-6 transsignalling in pancreatic oncogenesis. Through IL-6 transsignaling and Stat3, IL-6 promotes tumor development in the pancreas. Genetic manipulation of IL-6 transsignaling and Stat3 activation impairs PanIN formation and significantly impedes PDAC development. Using patient data and human PDAC specimens, we have demonstrated that this crosslink also exists in the human disease.

EXPERIMENTAL PROCEDURES

Mice

The LSL-$Kras^{G12D}$ knockin (Jackson et al., 2001), *Ptf1a-cre*^{ex1} (Nakhai et al., 2007), $Stat3^{F/F}$ (Sano et al., 1999), $sgp130^{tg}$ (Rabe et al., 2008), and $Socs3^{F/F}$ (Nakaya et al., 2009) strains were interbred to obtain compound mutant LSL-$Kras^{G12D}$;$Stat3^{F/F}$;*Ptf1a-cre*^{ex1} (termed $Kras^{G12D}$;$Stat3^{\Delta panc}$), LSL-$Kras^{G12D}$;*Ptf1a-cre*^{ex1};$sgp130tg$ (termed $Kras^{G12D}$;$sgp130^{tg}$), or LSL-$Kras^{G12D}$;$Socs3^{\Delta/\Delta}$;*Ptf1a-cre*^{ex1} (termed $Kras^{G12D}$;$Socs3^{\Delta panc}$) mice. LSL-$Kras^{G12D}$ (the negative control) and mutant LSL-$Kras^{G12D}$;*Ptf1a-cre*^{ex1} (termed $Kras^{G12D}$, the positive control) mice were used as control animals.

Il-6$^{-/-}$ (C57BL/6 background) mice were obtained from The Jackson Laboratory, Maine. LSL-$Kras^{G12D}$ knockin and *Il-6*$^{-/-}$ mice were interbred to generate LSL-$Kras^{G12D}$;*Il6*$^{-/-}$;*Ptf1a-cre*^{ex1} mice (termed $Kras^{G12D}$;*Il6*$^{-/-}$). All procedures conformed to the regulatory standards and were approved by the Regierung von Oberbayern.

Human Serum IL-6 Measurements

Serum samples were obtained from 38 patients with histologically or cytologically confirmed PDCA from whom pretreatment serum samples were available. The analysis group consisted of 15 females (median age 67 years, range 41–81 years) and 23 males (median age 68 years, range 50–80 years). Whole blood was collected prior to administration of chemotherapy. Serological analysis was performed at the Institute for Clinical Chemistry, Technical University, Munich. Control sera were obtained from healthy probands. The Local Ethics Committee approved the analysis, and written informed consent was obtained from all patients and controls.

Quantification of Proliferation, Apoptosis, and Inflammation

Mice were injected intraperitoneally with 50 mg/kg BrdU (Sigma) 2 hr prior to sacrifice, and paraffin sections were stained with anti-BrdU. Apoptosis was measured by immunohistochemistry of cleaved caspase-3. Inflammation was assessed using macrophage markers (F4/80). For each analysis, positive cells were scored in the pancreata from several animals of each genotype.

Flow Cytometry

Pancreata were injected with 1.2 mg/ml collagenase P (Roche) and minced. Single-cell suspensions of pancreatic cells were immunolabeled with fluorochrome-conjugated antibodies in PBS that was supplemented with 2% heat-inactivated FBS (Gibco-Invitrogen) and 5 mM EDTA (Sigma). All antibodies were purchased from eBioscience: eFluor 450-conjugated anti-CD45, fluorescein isothiocyanate-conjugated anit-CD19, PE-conjugated anti-F4/80, allophycocyanin-conjugated anti-CD11c, APC-eFluor 780-conjugated anti-CD11b, and Alexa Fluor 700-conjugated anti-CD3. Cells were stained with propidium iodide (BD Biosciences) to assess viability. Flow cytometry analysis was performed on a Gallios flow cytometer (Beckman Coulter) after gating and excluding dead cells. Data were analyzed using FlowJo software.

Statistical Analyses

Data are presented as averages ± standard deviaions (SD) and were analyzed by built-in t test using Microsoft Excel. $p < 0.05$ was considered significant. For the overall survival analysis, Kaplan-Meier curves were analyzed by log rank test. Tumor incidence was analyzed using Fisher's exact test. In all cases, we chose a group size that produced statistically unambiguous results.

SUPPLEMENTAL INFORMATION

Supplemental Information includes two table, four figures, and Supplemental Experimental Procedures and can be found with this article online at doi:10.1016/j.ccr.2011.03.009.

ACKNOWLEDGMENTS

We thank Karen Dlubatz for excellent technical assistance. M.U.K. is an MD/PhD candidate at the Technische Universität München. Y.A. received grants from the Ministry of Education, Culture, Sports, Science, and Technology of Japan, and the Program for Promotion of Fundamental Studies in Health Sciences of the National Institute of Biomedical Innovation. S.R.-J.

was supported by the Deutsche Forschungsgemeinschaft (SFB 877, TP A 1) and by the Cluster of Excellence "Inflammation at Interfaces." H.A. and R.M.S. were supported by the Deutsche Forschungsgemeinschaft (SFB 576, TP A 10 to H.A. and R.M.S), Deutsche Krebshilfe (Grant 10994 to H.A.), Else-Kröner-Fresenius-Stiftung (Grant 2010_A144 to H.A.), and by promotional programs of the Technische Universität München (KKF-C to H.A. and KKF-A to R.M.S). S.R.-J. is inventor on patents describing the function of sgp130Fc and is a shareholder of the CONARIS Research Institute (Kiel, Germany).

Received: June 23, 2010
Revised: December 1, 2010
Accepted: March 7, 2011
Published: April 11, 2011

REFERENCES

Aguirre, A.J., Bardeesy, N., Sinha, M., Lopez, L., Tuveson, D.A., Horner, J., Redston, M.S., and DePinho, R.A. (2003). Activated Kras and Ink4a/Arf deficiency cooperate to produce metastatic pancreatic ductal adenocarcinoma. Genes Dev. *17*, 3112–3126.

Algul, H., Treiber, M., Lesina, M., Nakhai, H., Saur, D., Geisler, F., Pfeifer, A., Paxian, S., and Schmid, R.M. (2007a). Pancreas-specific RelA/p65 truncation increases susceptibility of acini to inflammation-associated cell death following cerulein pancreatitis. J. Clin. Invest. *117*, 1490–1501.

Algul, H., Treiber, M., Lesina, M., and Schmid, R.M. (2007b). Mechanisms of disease: chronic inflammation and cancer in the pancreas–a potential role for pancreatic stellate cells? Nat. Clin. Pract. Gastroenterol. Hepatol. *4*, 454–462.

Algul, H., Wagner, M., Lesina, M., and Schmid, R.M. (2007c). Overexpression of ErbB2 in the exocrine pancreas induces an inflammatory response but not increased proliferation. Int. J. Cancer *121*, 1410–1416.

Barre, B., Vigneron, A., and Coqueret, O. (2005). The STAT3 transcription factor is a target for the Myc and riboblastoma proteins on the Cdc25A promoter. J. Biol. Chem. *280*, 15673–15681.

Bollrath, J., Phesse, T.J., von Burstin, V.A., Putoczki, T., Bennecke, M., Bateman, T., Nebelsiek, T., Lundgren-May, T., Canli, O., Schwitalla, S., et al. (2009). gp130-mediated Stat3 activation in enterocytes regulates cell survival and cell-cycle progression during colitis-associated tumorigenesis. Cancer Cell *15*, 91–102.

Chalaris, A., Rabe, B., Paliga, K., Lange, H., Laskay, T., Fielding, C.A., Jones, S.A., Rose-John, S., and Scheller, J. (2007). Apoptosis is a natural stimulus of IL6R shedding and contributes to the proinflammatory trans-signaling function of neutrophils. Blood *110*, 1748–1755.

Clark, C.E., Hingorani, S.R., Mick, R., Combs, C., Tuveson, D.A., and Vonderheide, R.H. (2007). Dynamics of the immune reaction to pancreatic cancer from inception to invasion. Cancer Res. *67*, 9518–9527.

Ebrahimi, B., Tucker, S.L., Li, D., Abbruzzese, J.L., and Kurzrock, R. (2004). Cytokines in pancreatic carcinoma: correlation with phenotypic characteristics and prognosis. Cancer *101*, 2727–2736.

Finco, T.S., Westwick, J.K., Norris, J.L., Beg, A.A., Der, C.J., and Baldwin, A.S., Jr. (1997). Oncogenic Ha-Ras-induced signaling activates NF-kappaB transcriptional activity, which is required for cellular transformation. J. Biol. Chem. *272*, 24113–24116.

Glienke, W., Maute, L., Wicht, J., and Bergmann, L. (2010). Curcumin inhibits constitutive STAT3 phosphorylation in human pancreatic cancer cell lines and downregulation of survivin/BIRC5 gene expression. Cancer Invest. *28*, 166–171.

Greten, F.R., Weber, C.K., Greten, T.F., Schneider, G., Wagner, M., Adler, G., and Schmid, R.M. (2002). Stat3 and NF-kappaB activation prevents apoptosis in pancreatic carcinogenesis. Gastroenterology *123*, 2052–2063.

Grivennikov, S., Karin, E., Terzic, J., Mucida, D., Yu, G.Y., Vallabhapurapu, S., Scheller, J., Rose-John, S., Cheroutre, H., Eckmann, L., and Karin, M. (2009). IL-6 and Stat3 are required for survival of intestinal epithelial cells and development of colitis-associated cancer. Cancer Cell *15*, 103–113.

Guerra, C., Schuhmacher, A.J., Canamero, M., Grippo, P.J., Verdaguer, L., Perez-Gallego, L., Dubus, P., Sandgren, E.P., and Barbacid, M. (2007). Chronic pancreatitis is essential for induction of pancreatic ductal adenocarcinoma by K-Ras oncogenes in adult mice. Cancer Cell *11*, 291–302.

He, G., Yu, G.Y., Temkin, V., Ogata, H., Kuntzen, C., Sakurai, T., Sieghart, W., Peck-Radosavljevic, M., Leffert, H.L., and Karin, M. (2010). Hepatocyte IKKbeta/NF-kappaB inhibits tumor promotion and progression by preventing oxidative stress-driven STAT3 activation. Cancer Cell *17*, 286–297.

Hidalgo, M. (2010). Pancreatic cancer. N. Engl. J. Med. *362*, 1605–1617.

Hingorani, S.R., Petricoin, E.F., Maitra, A., Rajapakse, V., King, C., Jacobetz, M.A., Ross, S., Conrads, T.P., Veenstra, T.D., Hitt, B.A., et al. (2003). Preinvasive and invasive ductal pancreatic cancer and its early detection in the mouse. Cancer Cell *4*, 437–450.

Hingorani, S.R., Wang, L., Multani, A.S., Combs, C., Deramaudt, T.B., Hruban, R.H., Rustgi, A.K., Chang, S., and Tuveson, D.A. (2005). Trp53R172H and KrasG12D cooperate to promote chromosomal instability and widely metastatic pancreatic ductal adenocarcinoma in mice. Cancer Cell *7*, 469–483.

Hruban, R.H., Adsay, N.V., Albores-Saavedra, J., Anver, M.R., Biankin, A.V., Boivin, G.P., Furth, E.E., Furukawa, T., Klein, A., Klimstra, D.S., et al. (2006). Pathology of genetically engineered mouse models of pancreatic exocrine cancer: consensus report and recommendations. Cancer Res. *66*, 95–106.

Hutzen, B., Friedman, L., Sobo, M., Lin, L., Cen, L., De Angelis, S., Yamakoshi, H., Shibata, H., Iwabuchi, Y., and Lin, J. (2009). Curcumin analogue GO-Y030 inhibits STAT3 activity and cell growth in breast and pancreatic carcinomas. Int. J. Oncol. *35*, 867–872.

Jackson, E.L., Willis, N., Mercer, K., Bronson, R.T., Crowley, D., Montoya, R., Jacks, T., and Tuveson, D.A. (2001). Analysis of lung tumor initiation and progression using conditional expression of oncogenic K-ras. Genes Dev. *15*, 3243–3248.

Kawesha, A., Ghaneh, P., Andren-Sandberg, A., Ograed, D., Skar, R., Dawiskiba, S., Evans, J.D., Campbell, F., Lemoine, N., and Neoptolemos, J.P. (2000). K-ras oncogene subtype mutations are associated with survival but not expression of p53, p16(INK4A), p21(WAF-1), cyclin D1, erbB-2 and erbB-3 in resected pancreatic ductal adenocarcinoma. Int. J. Cancer *89*, 469–474.

Kelly, K.A., Bardeesy, N., Anbazhagan, R., Gurumurthy, S., Berger, J., Alencar, H., Depinho, R.A., Mahmood, U., and Weissleder, R. (2008). Targeted nanoparticles for imaging incipient pancreatic ductal adenocarcinoma. PLoS Med. *5*, e85.

Kim, D., Sun, M., He, L., Zhou, Q.H., Chen, J., Sun, X.M., Bepler, G., Sebti, S.M., and Cheng, J.Q. (2010). A small molecule inhibits Akt through direct binding to Akt and preventing Akt membrane translocation. J. Biol. Chem. *285*, 8383–8394.

Kocher, H.M., Mears, L., Lea, N.C., Raj, K., and Mufti, G.J. (2007). JAK V617F missense mutation is absent in pancreatic cancer. Gut *56*, 1174–1175.

Kurahara, H., Shinchi, H., Mataki, Y., Maemura, K., Noma, H., Kubo, F., Sakoda, M., Ueno, S., Natsugoe, S., and Takao, S. (2009). Significance of M2-polarized tumor-associated macrophage in pancreatic cancer. J. Surg. Res., in press. Published online June 16, 2009. 10.1016/j.jss2009.05.026.

Lin, J., Jin, X., Rothman, K., Lin, H.J., Tang, H., and Burke, W. (2002). Modulation of signal transducer and activator of transcription 3 activities by p53 tumor suppressor in breast cancer cells. Cancer Res. *62*, 376–380.

Lin, L., Hutzen, B., Li, P.K., Ball, S., Zuo, M., DeAngelis, S., Foust, E., Sobo, M., Friedman, L., Bhasin, D., et al. (2010a). A novel small molecule, LLL12, inhibits STAT3 phosphorylation and activities and exhibits potent growth-suppressive activity in human cancer cells. Neoplasia *12*, 39–50.

Lin, L., Hutzen, B., Zuo, M., Ball, S., Deangelis, S., Foust, E., Pandit, B., Ihnat, M.A., Shenoy, S.S., Kulp, S., et al. (2010b). Novel STAT3 phosphorylation inhibitors exhibit potent growth-suppressive activity in pancreatic and breast cancer cells. Cancer Res. *70*, 2445–2454.

Lowenfels, A.B., Maisonneuve, P., Cavallini, G., Ammann, R.W., Lankisch, P.G., Andersen, J.R., Dimagno, E.P., Andren-Sandberg, A., and Domellof, L. (1993). Pancreatitis and the risk of pancreatic cancer. International Pancreatitis Study Group. N. Engl. J. Med. *328*, 1433–1437.

Luttges, J., Neumann, S., Jesnowski, R., Borries, V., Lohr, M., and Kloppel, G. (2003). Lack of apoptosis in PanIN-1 and PanIN-2 lesions associated with pancreatic ductal adenocarcinoma is not dependent on K-ras status. Pancreas *27*, e57–e62.

Marrache, F., Tu, S.P., Bhagat, G., Pendyala, S., Osterreicher, C.H., Gordon, S., Ramanathan, V., Penz-Osterreicher, M., Betz, K.S., Song, Z., and Wang, T.C. (2008). Overexpression of interleukin-1beta in the murine pancreas results in chronic pancreatitis. Gastroenterology *135*, 1277–1287.

Masuda, M., Suzui, M., Yasumatu, R., Nakashima, T., Kuratomi, Y., Azuma, K., Tomita, K., Komiyama, S., and Weinstein, I.B. (2002). Constitutive activation of signal transducers and activators of transcription 3 correlates with cyclin D1 overexpression and may provide a novel prognostic marker in head and neck squamous cell carcinoma. Cancer Res. *62*, 3351–3355.

Matthews, V., Schuster, B., Schutze, S., Bussmeyer, I., Ludwig, A., Hundhausen, C., Sadowski, T., Saftig, P., Hartmann, D., Kallen, K.J., and Rose-John, S. (2003). Cellular cholesterol depletion triggers shedding of the human interleukin-6 receptor by ADAM10 and ADAM17 (TACE). J. Biol. Chem. *278*, 38829–38839.

Nakaya, M., Hashimoto, M., Nakagawa, R., Wakabayashi, Y., Ishizaki, T., Takada, I., Komai, K., Yoshida, H., and Yoshimura, A. (2009). SOCS3 in T and NKT cells negatively regulates cytokine production and ameliorates ConA-induced hepatitis. J. Immunol. *183*, 7047–7053.

Nakhai, H., Sel, S., Favor, J., Mendoza-Torres, L., Paulsen, F., Duncker, G.I., and Schmid, R.M. (2007). Ptf1a is essential for the differentiation of GABAergic and glycinergic amacrine cells and horizontal cells in the mouse retina. Development *134*, 1151–1160.

Rabe, B., Chalaris, A., May, U., Waetzig, G.H., Seegert, D., Williams, A.S., Jones, S.A., Rose-John, S., and Scheller, J. (2008). Transgenic blockade of interleukin 6 transsignaling abrogates inflammation. Blood *111*, 1021–1028.

Reid, T., Jin, X., Song, H., Tang, H.J., Reynolds, R.K., and Lin, J. (2004). Modulation of Janus kinase 2 by p53 in ovarian cancer cells. Biochem. Biophys. Res. Commun. *321*, 441–447.

Rose-John, S., and Heinrich, P.C. (1994). Soluble receptors for cytokines and growth factors: generation and biological function. Biochem. J. *300*, 281–290.

Rose-John, S., Scheller, J., Elson, G., and Jones, S.A. (2006). Interleukin-6 biology is coordinated by membrane-bound and soluble receptors: role in inflammation and cancer. J. Leukoc. Biol. *80*, 227–236.

Sano, S., Itami, S., Takeda, K., Tarutani, M., Yamaguchi, Y., Miura, H., Yoshikawa, K., Akira, S., and Takeda, J. (1999). Keratinocyte-specific ablation of Stat3 exhibits impaired skin remodeling, but does not affect skin morphogenesis. EMBO J. *18*, 4657–4668.

Sawai, H., Funahashi, H., Matsuo, Y., Yamamoto, M., Okada, Y., Hayakawa, T., and Manabe, T. (2003). Expression and prognostic roles of integrins and interleukin-1 receptor type I in patients with ductal adenocarcinoma of the pancreas. Dig. Dis. Sci. *48*, 1241–1250.

Scholz, A., Heinze, S., Detjen, K.M., Peters, M., Welzel, M., Hauff, P., Schirner, M., Wiedenmann, B., and Rosewicz, S. (2003). Activated signal transducer and activator of transcription 3 (STAT3) supports the malignant phenotype of human pancreatic cancer. Gastroenterology *125*, 891–905.

Sipos, B., Moser, S., Kalthoff, H., Torok, V., Lohr, M., and Kloppel, G. (2003). A comprehensive characterization of pancreatic ductal carcinoma cell lines: towards the establishment of an in vitro research platform. Virchows Arch. *442*, 444–452.

Talar-Wojnarowska, R., Gasiorowska, A., Smolarz, B., Romanowicz-Makowska, H., Kulig, A., and Malecka-Panas, E. (2009). Clinical significance of interleukin-6 (IL-6) gene polymorphism and IL-6 serum level in pancreatic adenocarcinoma and chronic pancreatitis. Dig. Dis. Sci. *54*, 683–689.

Trevino, J.G., Gray, M.J., Nawrocki, S.T., Summy, J.M., Lesslie, D.P., Evans, D.B., Sawyer, T.K., Shakespeare, W.C., Watowich, S.S., Chiao, P.J., et al. (2006). Src activation of Stat3 is an independent requirement from NF-kappaB activation for constitutive IL-8 expression in human pancreatic adenocarcinoma cells. Angiogenesis *9*, 101–110.

Yu, H., Pardoll, D., and Jove, R. (2009). STATs in cancer inflammation and immunity: a leading role for STAT3. Nat. Rev. Cancer *9*, 798–809.